A 37 years hindcast of a coupled physical-biogeochemical model and its use for fisheries oceanography in the Bay of Biscay

M. Huret[1], P. Petitgas[1], C. Struski[1], F. Léger[3], M. Sourisseau[2] and P. Lazure[2]

Overexploitation and climate change are increasingly causing unanticipated changes in marine ecosystems, such as higher variability in fish recruitment and shifts in species distribution, pressing for developing fisheries oceanography. In the meantime, operational oceanography rapidly progresses and its products become easy to access to a large community, among them fisheries scientists. Multiyear oceanographic reanalyses (hindcasts) were identified has a priority product by the ICES WG on Operational Oceanographic Products for Fisheries and Environment (WGOOFE). We performed a 37 years hindcast (1972-2008) run with a coupled physical-biogeochemical model (ECO-MARS3D) over the Bay of Biscay, using realistic meteorological and run-off forcing.

We first describe the coupled model, as well as the mesoscale and biological indices that were derived as potential drivers of fish populations. Then we use a Multiple Factorial Analysis (MFA) allowing for a synthetic characterization of the seasonal variability of the environment in the Bay of Biscay, based on the whole set of indices. We also rapidly go through the main trends detected by the hindcast over the last decades. Last, we review the different use we made from this hindcast in relation to anchovy life cycle in the Bay of Biscay. These applications range from forcing higher trophic level models, to fish habitat statistical modelling relating egg or adult field distribution to environment covariates, and to finally testing the ability of integrated indices in explaining the recruitment variability.

[1] IFREMER, Centre de Nantes, BP 21105, 44311 Cedex 03, Nantes, France
[2] IFREMER, Centre de Brest, BP 70, 29280, Plouzané, France
[3] LEGOS/OMP, 14, Av. Edouard Belin - 31400 Toulouse, France

Contact author: Martin Huret, martin.huret@ifremer.fr

1 Introduction

There is a growing interest in continuously monitoring the ocean state, from surface to bottom layers and over several decades from past to future, with the need to understand and anticipate the effect of climate change on marine biogeochemistry and resources. Satellite remotely sensed data has already shown its potential in deriving ecosystem indicators (Polovina and Howell, 2005; Chassot et al., in revision), however time coverage is obviously limited back in time, and spatial coverage is mainly limited to the ocean surface layers. Coupled physical-biological models provide extensive source of information on both the physical and biological state of the ocean in its four dimension, without any temporal limitation, as soon as the forcing are available and now that computing power become less and less a limiting factor. Also an extensive list of oceanographic or ecosystem indicators may be derived from these models. The applications of the coupled model products range from the assessment of a reference state of the marine environment, as necessary for the Marine Strategy Framework Directive (Anonymous, 2008), to the detection of trends related to climate change, and to the Ecosystem Approach to Fisheries (Cury *et al.*, 2008).

In this paper we present the hindcast of a physical-biogeochemical model (ECOMARS) over the Bay of Biscay, run over a 37 years period (1972-2008). The model is a N3-P3-Z2-D type model, simulating the dynamics of pico-nanoplankton, diatoms and dinoflagellates, under the limitations of nitrogen, silicates and phosphates, and of micro- and meso-zooplankton. The model is forced by realistic high-frequency meteorological and river discharge/loads forcing.

The oceanography of the Bay of Biscay is not forced by one major driver and is best characterized by a variety of mesoscale features that can be active depending on the climate and seasonal conditions (Koutsikopoulos and Le Cann, 1996). Typically, mesoscale structures range from tens to a few hundred kilometres and last from a few weeks to months. Mesoscale structures are highly energetic and are often associated with areas of strong biological activity under the Bakun's fundamental triad (Bakun, 1996) processes (enrichment, retention and concentration). As such they act as a potentially dominant controlling force on marine populations. So, in addition to model state variables, we derived a suite of indices describing the mesoscale activity and biological production in the Bay of Biscay. The set of mesoscale indices describe the depth and strength of stratification, location of fronts, eddies and upwellings, and extension of river plumes. Biological production is provided through the vertically integrated primary production. As a whole, the hindcast provides half of the variables listed as useful by the WGOOFE, and among them the eight most requested variables by the ICES community (Berx et al., in prep.).

The present paper aims at presenting the model and the construction of the associated oceanographic indices. The model and some of its derived indices has already shown its potential for statistical monitoring of the environment (Woillez et al., 2010), taking into account deviance from reference spatial patterns based on EOF analysis. Here we present an overview of the Bay of Biscay ecosystem as seen by our model and derived indices, presenting the major information that can be drawn from the hindcast on seasonal variability and multi-annual trend, and without considering the spatial patterns. We also review the applications of such a product for fisheries oceanography studies.

2 Model description

The hydrodynamic model

The hydrodynamic component of our coupled model is the model MARS (hydrodynamic Model for Application at Regional Scale; Lazure and Dumas, 2008). The model was set up over the Bay of Biscay area and validated for tide and hydrology (Lazure and Dumas, 2008; Lazure et al., 2009). The geographic domain of the 3D model extends from 43.2ºN to 50.8ºN, and from 8ºW to 0.4ºW, covering the whole Bay of Biscay and the western English Channel (Fig. 1). It uses a 4 km horizontal regular grid, with 30 sigma layers in the vertical with refinement in the surface layers. A 2D model is run over a larger area (from Portugal to Norway) to provide surface elevation to the 3D model boundaries. A

total of eight tidal constituents along the open boundary of the large model were extracted from FES2004 (Lyard et al. 2006).
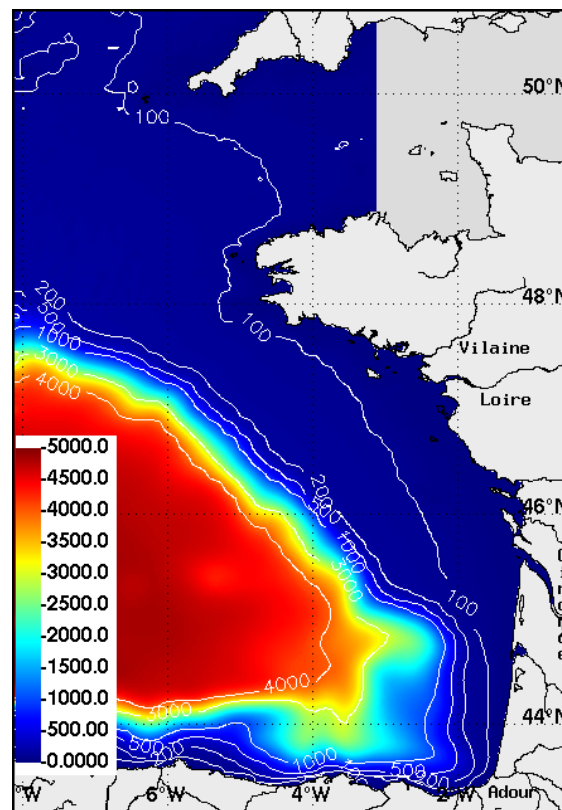

Fig.1 Model domain with bathymetry and rivers.

The biogeochemical model

The model MARS is coupled to a biogeochemical model (Fig. 2) describing the seasonal evolution of primary production by diatoms, dinoflagellates and pico-nanoplankton, with limitations by nitrates, ammonium, phosphates and silicates. We model two zooplankton compartments, microzooplankton and mesozooplankton, the latter being the closure term of our model. This model results from successive coupled model works over the Bay of Biscay (Loyer, 2001; Huret et al., 2007) or local areas within the Bay (Chapelle, 1994, Le Pape et al., 1997; Ménesguen et al., 2006). The turbidity being high during stormy winter months, we constrain the light availability for primary production from a climatology of satellite derived Suspended Particulate Matter (see Huret et al., 2007) .
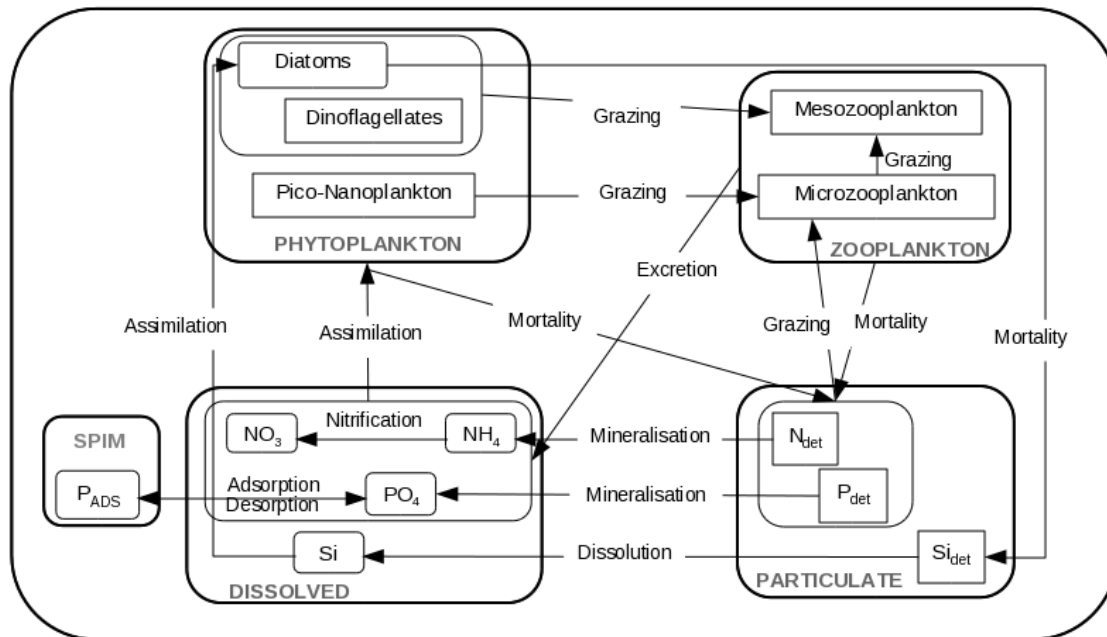
Fig.2. The biogeochemical model with its state variables.

Hindcast configuration

The model is run over the period 1972-2009 with realistic meteorological and run-off forcing and outputs are saved on a three day basis. Atmospheric forcing (wind fields, air temperature, atmospheric pressure, cloud cover and relative humidity) are provided by ERA (1.125° and 6h resolution) for the period 1971-1995 and from the Météo-France model ARPEGE (0.5° and 6h resolution) for the most recent years. Bulk formulae are used for heat fluxes calculations. Daily river discharges from the Loire, Gironde, Adour and Vilaine rivers are input. For these rivers, concentrations in ammonium, nitrates, silicium and phosphates, as well as the organic part of these elements as detritus are provided. These concentrations were calculated based on regression analysis between river run-off and loads when data available (Guillaud, 2008).
Boundary conditions for temperature and salinity are provided by the Reynaud climatology (Reynaud, 1998). Climatological data from the Levitus atlas (Levitus et al., 1998) provide boundary conditions in chlorophyll-a and nutrients.

3   The derived indices (2D maps)

From the raw model variables, we derived 2D maps of relevant hydrological indices to further characterise the physical and biological environment. These are listed in Table 1 and detailed below. They are calculated on the same spatial and temporal resolution as the model outputs.
The maximum depth considered when calculating depth-integrated values or when measuring gradients in the vertical dimension is 60m, except for the depth-integrated primary production which is integrated over the whole water column.

Table 1. List of hydrological indices (2D) compiled from the ECO-MARS3D raw data.

Hydrological indices	Units
Stratification indices	
Deficit of potential energy (Density)	kg.m^{-1}.s^{-2}
Deficit of potential energy (temperature)	kg.m^{-1}.s^{-2}
Maximal vertical gradient in density	kg.m^{-3}.m^{-1}
Maximal vertical gradient in temperature	°C.m^{-1}
Depth of thermocline	m
Depth of pycnocline	m
Depth of halocline	m
Frontal indices	
Thermal frontal index (potential energy)	kg.m^{-2}.s^{-2}
Density frontal index (potential energy)	kg.m^{-2}.s^{-2}
Thermal frontal index (maximal gradient)	°C.m^{-2}
Density frontal index (maximal gradient)	kg.m^{-3}.m^{-2}
Upwelling indices	
Vertical speed in σ coordinates	s^{-1}
Vertical speed in z coordinates	m.d^{-1}
River plume indices	
Salinity at surface (3m)	psu
Equivalent fresh water height	m
Eddies indices	
Vorticity	s^{-1}
Okubo-Weiss	s^{-2}
Biological indices	
Surface chlorophylle (chla) concentration (at 3m)	mgChla.m^{-3}
Primary production over 3 days	gC.m^{-2}
Other indices	
Temperature at surface (3m)	°C
Temperature at the bottom	°C
Current U-component (W-E) at the surface (10m)	m.s^{-1}
Current V-component (S-N) at the surface (10m)	m.s^{-1}

Stratification indices

The deficit of potential energy

This is the necessary energy to homogenize density of the water column and is defined as:

$$Def.pot = \frac{1}{H+\xi} \int_{-H}^{\xi} \left(\bar{\rho} - \rho_z \right) gz dz$$

with $\bar{\rho}$ the mean density over the water column $\bar{\rho} = \frac{1}{H+\xi} \int_{-H}^{\xi} \rho_z dz$, ρ_z the density at depth z, *H* the bathymetry and ξ the height of the free surface.

The density is calculated as a function of temperature and salinity, or only temperature in case the focus is on temperature stratification.
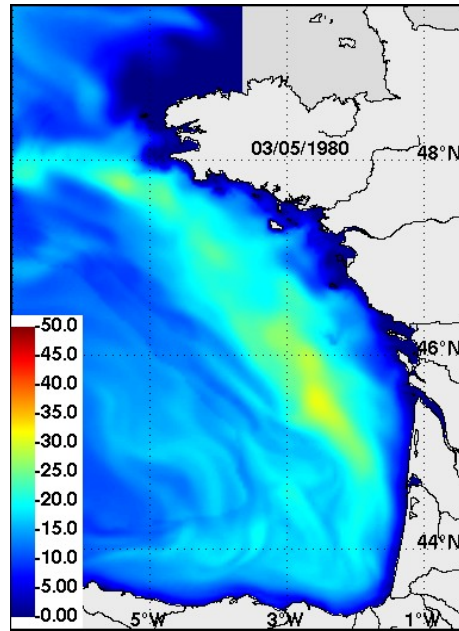
Fig. 3. Snapshot of thermal stratification from deficit of potential energy (kg.m^{-1}.s^{-2}).

Maximum vertical gradient
This stratification index is the maximum vertical gradient of temperature or density.

Depth of thermocline, halocline and pycnocline

The depth of a cline is defined as the depth where the maximum gradient is found. It is calculated for values higher than the following thresholds: 0.15°C.m^{-1}, 0.05 kg.m^{-3}.m^{-1} and 0.1 m^{-1} for temperature, density and salinity, respectively.

Frontal indices

The indices of frontal activity are based on the maximum horizontal gradient of the stratification indices. Frontal indices from vertical gradient as well as from deficit of potential energy are then calculated.

For example, the frontal index from the maximum vertical gradient in temperature is given by:

$$FT = \frac{1}{2} max \left(\frac{|Strat_{i+1,j} - Strat_{i-1,j}|}{2dx}, \frac{|Strat_{i,j+1} - Strat_{i,j-1}|}{2dy} \right)$$ with Strat one of the stratification index, and respectively dx and dy the longitudinal and latitudinal resolution of the model.
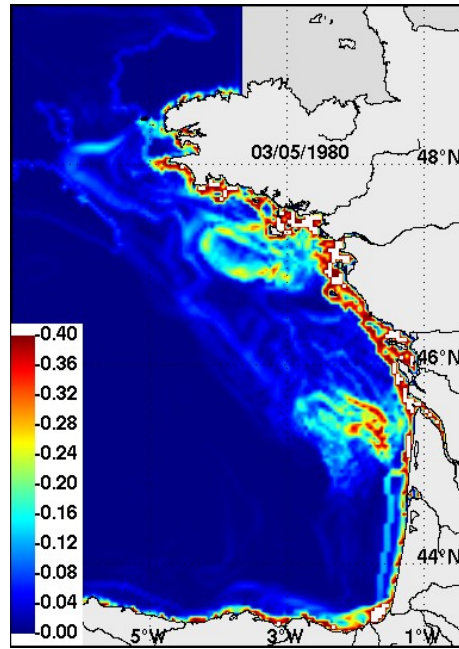
Fig. 4: Snapshot of the front index from maximum vertical gradient of density ($\times 10^{-4}$ kg.m^{-3}.m^{-2}).

Upwelling index

This is the integration of vertical velocities in sigma coordinates over the whole water column:

$$Upwelling = \sum_{0}^{nz} \tilde{\omega} \quad \text{with nz the number of vertical layers.}$$

River plume indices

These indices highlight the horizontal extension of the river plumes. The first index is the surface salinity, given at a depth of 3m. Second index is the equivalent freshwater depth following Choi (2007):

$$Equivalent\ freshwater\ depth = \int_{-H}^{\xi} \frac{S_0 - S_z}{S_0} dz \quad \text{with } S_0 \text{ a reference salinity taken as 35.5.}$$

This quantity allows direct estimation of the plume depth in addition to its horizontal extension.
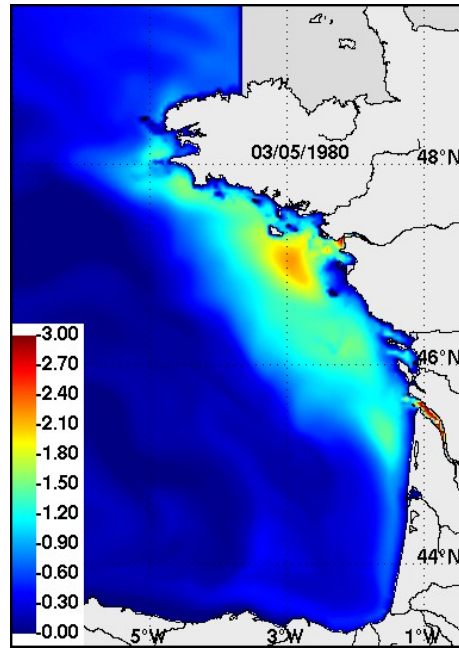
Fig. 5: Snapshot of equivalent freshwater depth (in meter).

Eddy indices

The eddy indices are calculated for a detph of 10m.

Vorticity.
The vorticity index measures the fluid rotation, with positive or negative values in the cyclonic, or anticyclonic direction, respectively.

$\omega = \dfrac{\partial v}{\partial x} - \dfrac{\partial u}{\partial y}$ with u and v the horizontal components of the velocity field, x and y the horizontal coordinates.

Okubo-Weiss index.
This index allows detection of the limits of eddies (Insern-Fontanet, 2006) and is calculated as:

$Okubo = \left(\dfrac{\partial u}{\partial x} - \dfrac{\partial v}{\partial y} \right)^2 + \left(\dfrac{\partial v}{\partial x} + \dfrac{\partial u}{\partial y} \right)^2 - \left(\dfrac{\partial v}{\partial x} - \dfrac{\partial u}{\partial y} \right)^2$

First two terms represent the shear stress and last term vorticity. Eddies are characterised by a strong vorticity in their center and a large shear stress deformation at their boundaries. Eddies are then detected by negative Okubo-Weiss values enclosed by positive values.
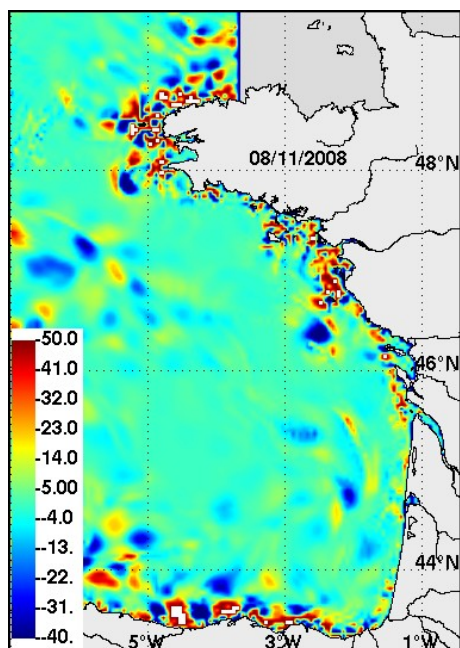
Fig. 6: Snapshot of the eddy index from Okubo-Weiss at 10m depth ($\times 10^{-12}.s^{-2}$).

Biological indices

From raw biological values, we derived the chlorophyll concentration, as the sum of nitrogen concentrations of diatoms, dinoflagellates and pico-nanoplankton considering a Redfield C/N ratio of 6.625 and a gChl/gC ratio of 50. Surface chlorophyll-a is provided for a depth of 3m. The integrated primary production over the whole water column and cumulated over the output frequency, i.e. 3 days, is also calculated as the sum of production from the three phytoplankton components.
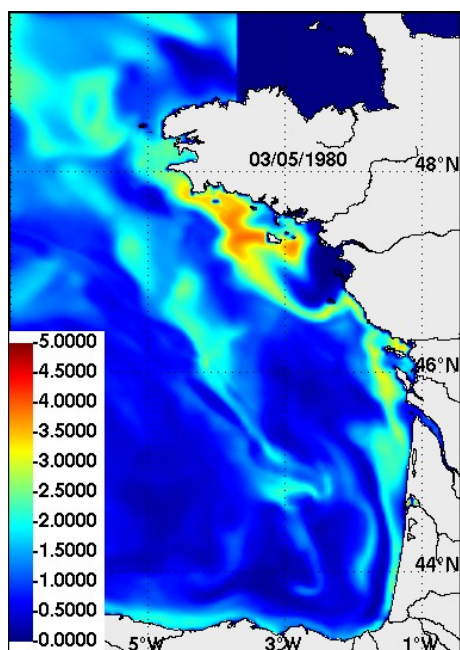

Fig. 7: Snapshot of the integrated primary production ($gC.m^{-2}.day^{-1}$).

The integrated 1D indices

From 2D maps of raw data or derived indices (Table 2), we also calculated monthly and spatially averaged or cumulated values of indices, to study the seasonal and interannual variability in the environment. The list of proposed averaged indices is given in Table 3. These integrated indices are mostly averaged values of raw or derived indices. Specific cases apply to areas which are calculated

considering threshold values, as well as to upwelling and eddy indices. For stratified areas, the condition is that thermocline or pycnocline is established. For plume area, the threshold are 34 and 1 meter when considering surface salinity and equivalent freshwater depth, respectively. The Okubo-Weiss area represents the surface covered by eddies, with an upper threshold of -10E-12 for the Okubo-Weiss criterion and after removal of small structures (i.e. less than 4 grid cells). For bloom area, the chlorophyll-a threshold value is 3 mg.m^3. The upwelling integrated index is the sum of positive values of upwelling after averaging them within the 50m isobath.

Table 2. List of 1D monthly averaged indices with threshold values to calculate areas.

Integrated indices	Units	Threshold value
Surface temperature (3m)	°C	
Bottom temperature	°C	
Thermocline depth	m	
Pycnocline depth	m	
Deficit of potential energy	kg.m^{-2}.s^{-2}	
Stratified area (thermocline)	km^2	0.15 °C.m^{-1}
Stratified area (pycnocline)	km^2	0.05 kg.m^{-3}.m^{-1}
Equivalent fresh water height	m	
Plume area (surface salinity)	km^2	34 psu
Plume area (equivalent fresh water height)	km^2	1 meter
Thermal frontal index (potential energy)	kg.m^{-2}.s^{-2}	
Upwelling index	m	
Okubo-Weiss (eddies) area	km^2	-10E^{-12} s^{-2}
Surface chlorophylle concentration (at 3m)	mgChla.m^{-3}	
Bloom area	km^2	3 mgChla.m^{-3}
Primary production	gC.m^{-2}	

4 Characterisation of the seasonal pattern based on the integrated indices

A Multiple Factor analysis (MFA) was already applied by Petitgas et al. (2009) on the EOF amplitudes of several variables output from our Bay of Biscay hindcast, to test the matching with the schedule of anchovy life cycle. Here we proceed with a MFA on a completed set of spatially integrated indices as described in previous section, thus without consideration of the spatial patterns.

Multiple Factor analysis is applied on the monthly averaged indices to characterize the seasonal pattern in all the environment variables and the variability across years around that pattern. MFA proceeds as a two-step PCA. First, a PCA is applied to each yearly matrix (indices in column and months in row), and each column is standardized by the first eigen value. This step scales the yearly matrices so that all have a similar weight in the analysis. Then a PCA is performed on an overall matrix obtained by appending all the yearly matrices column by column. For doing so we used the library ade4 in R (Dray and Dufour, 2007). The MFA resulted in constructing a factorial space common to all yearly matrices in which all variables (i.e. indices) and years were represented. The MFA factorial space characterized the average correlation structure between indices and the principal factors of the MFA were interpreted by the correlation of each index with the factors. The seasonal cycle was characterized in that way. The variability between years for each month was represented as well as the distance of each year to the mean seasonal pattern. The variability in each month was measured by the sum over the years of the square distance between each yearly point and the mean monthly point in the MFA factorial space.

A strong seasonal cycle is identified for the Bay of Biscay (Fig.8). In general, the inter-annual variability within each month is less than the inter-month variability. However some months formed clusters in which inter-annual and inter-month variability were similar, meaning high consistency for these periods in the reproducibility of the correlation between indices. This high consistency occurred for summer and winter months.

Some months showed higher inertia than others and the indices involved for these months were also more variable (Fig. 9). Summer months and February were the less variable periods across years. Early spring was the most variable period and plume extension was the major parameter involved in that period (Fig. 9; see also indices correlation with axis 2 in Table 3). Not surprisingly surface temperature, but also stratification and frontal activity separate summer and winter months, whereas highest bottom temperature characterises autumn months. Bloom activity associated with high primary production is the specificity of late spring. Summing up, the first principal axis expresses the seasonal difference between summer and winter with the indices associated to surface temperature, stratification and primary production. The second principal axis expresses the seasonal difference between spring and autumn in terms of river plumes and bottom temperature, and to a lesser extent also in terms of upwelling and bloom activity (spring) and surface covered by eddy activity (end of autumn).

The MFA also provides the distance of the years to the mean seasonal pattern (Fig. 9). The method extracts singular years (1974, 1988, 1994, 1997 and 2007-2008) from the years close to the average pattern (1973, 1979, 1985, 1989), mostly located in the seventies and eighties. This reveals a general increase after the early nineties of the distance to the mean pattern, meaning more chance for particular or extreme years in the recent past period.
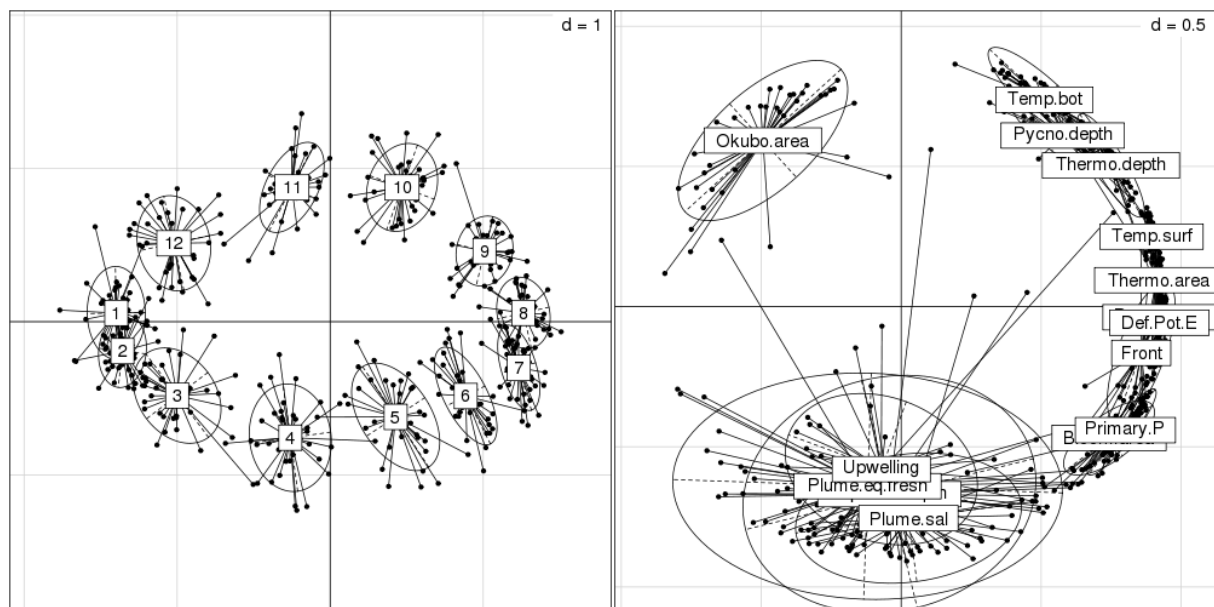

Fig. 8. Seasonal pattern : representation of the mean individuals (months: left) and indices (correlation circles : right) in the MFA subspace of the 2 first principal axes. Each point represents a particular year.

Table 3. Interpretation of the MFA principal components. Number of years in which the correlation between each index and the PC is >0.5 (in absolute value). The sign of the correlation is noted after the count.

| Integrated indices	First axis		Second axis	
Surface temperature (3m)	37+	0-	0+	0-
Bottom temperature	20+	0-	36+	0-
Thermocline depth	36+	0-	22+	0-
Pycnocline depth	25+	0-	32+	0-
Deficit of potential energy	37+	0-	0+	0-
Stratified area (thermocline)	37+	0-	0+	0-
Stratified area (pycnocline)	37+	0-	0+	0-
Equivalent fresh water height	2+	4-	1+	31-
Plume area (surface salinity)	0+	0-	0+	36-
Plume area (equivalent fresh water height)	7+	10-	0+	31-
Thermal frontal index (potential energy)	37+	0-	0+	1-
Upwelling index	1+	0-	0+	28-
Okubo-Weiss (eddies) area	0+	17-	25+	0-
Surface chlorophylle concentration (at 3m)	37+	0-	0+	10-
Bloom area	36+	0-	0+	14-
Primary production	37+	0-	0+	7-
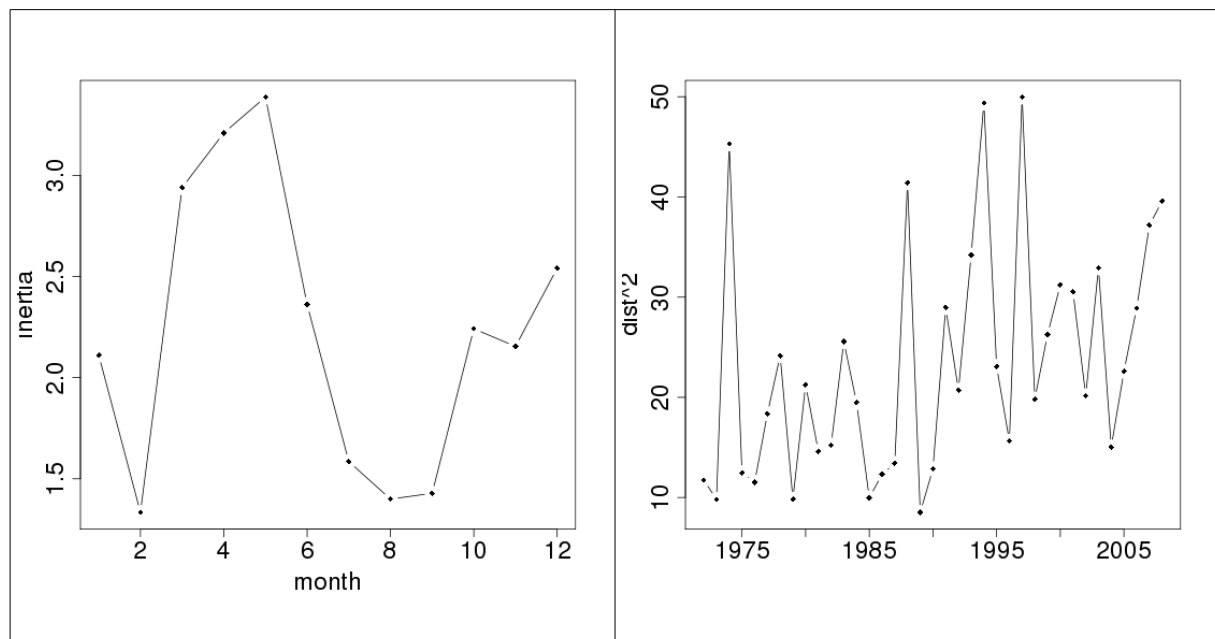
Fig. 9. Variability across years: inertia for each month (left) and distance to the mean seasonal pattern for each year (right) over the Bay of Biscay shelf, as derived from the MFA.

5   Trends in the environment

Fig. 10a shows the warming trend over the Bay of Biscay. Not surprisingly 2003 is the warmest year based on surface temperature, with 2006 in second position. This feature is more obvious at surface than in the bottom layer (not shown), which shows higher variability. But even with two recent years with cold bottom temperature (2005 and 2006), warmest years for bottom temperatures are still included in the last decade. Surface warming (0.336°C/decade, p<0.01) since the mid-eighties is comparable with what is observed from *in-situ* data (0.3°C/decade) and satellite SST images (0.36°C/decade) (Michel et al., 2009). When considering the whole hindcasted period, the trend is

lower (0.165°C/decade, p<0.001), revealing an increasing warming in the most recent decades.

Plume surface is strongly correlated with river discharge but will also depend on how plumes disperse in the horizontal and mix with deeper layers over the shelf. Considering the freshwater equivalent depth rather than salinity give less weight to the mixing as it considers the cumulated freshwater quantity over the water column. The plume surface shows a periodic oscillation (Fig. 10b), with two main peaks in the early 1980s and 2000s, and high variability between 1994-1995 and 1996-1998.

The annual primary production is given as a productivity index (Figure 10c). 1970s were average productive years, whereas 1980s were low productive years. In general, after a decreasing trend in the productivity from early 1970s to the mid-eighties, the trend is on the increase until most recent years. Whether this is a model artefact or a real trend related to the general warming or river loads is under investigation.
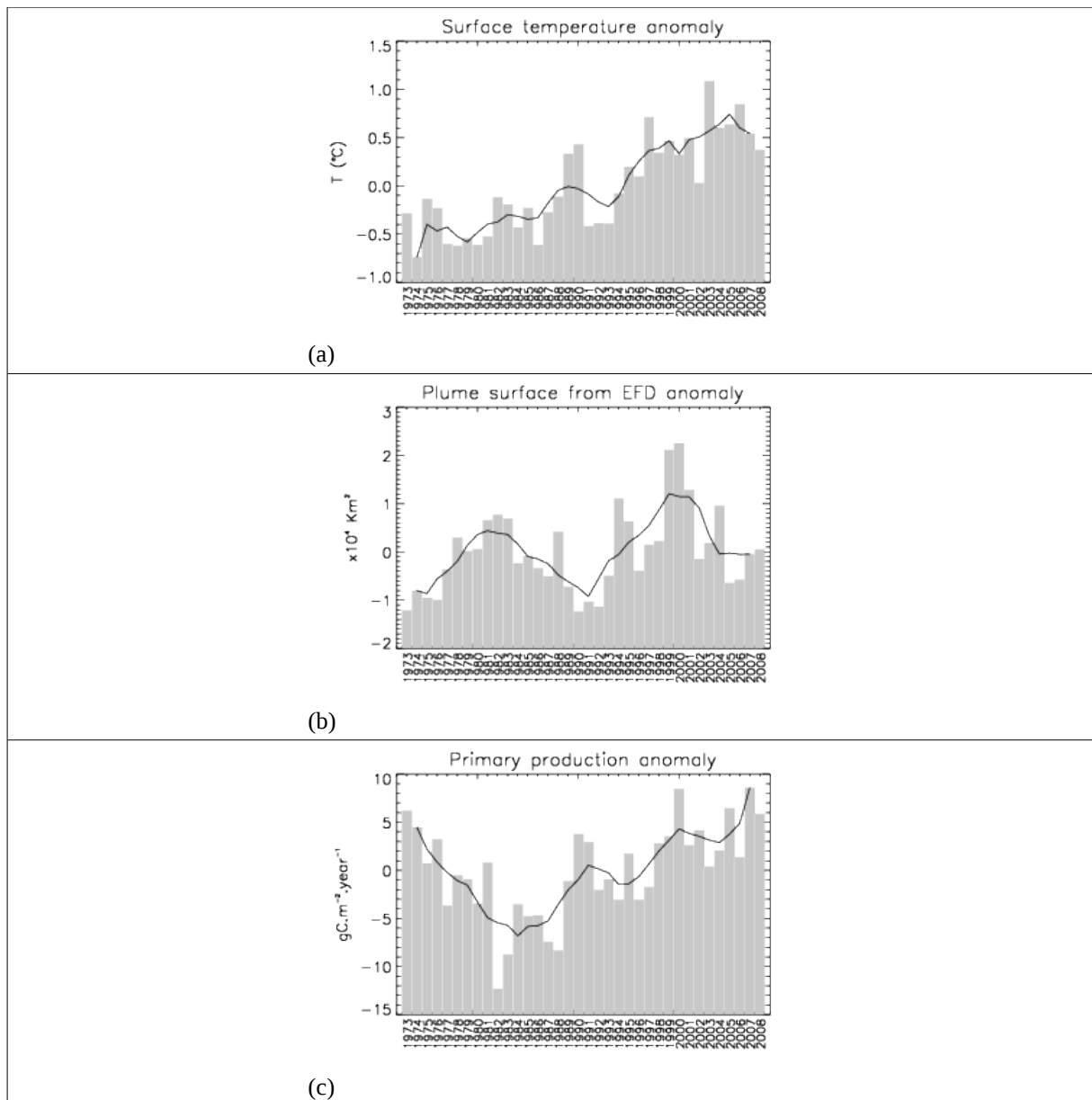
Fig. 10. Time-series and trend in the annual anomalies of surface temperature (a), plume surface (b) and primary production (c).

6 Overview of potential applications for fisheries oceanography

The hindcast performed for the Bay of Biscay is the first product of this type over the region, providing the most requested variables by fisheries scientist (Berx et al., in prep.), among them model raw variables such as temperature, salinity, nutrients and chlorophyll, but also mesoscale features and primary productivity. Other variables such as turbulence, bed shear-stress or secondary production would be easily available in future version of such a hindcast, even if further validation would be required especially for biological components. Other variables required by end-users such as fish larval distribution would require further model development, even if some early products only based on larval drift (Huret et al., 2010) could be delivered as a first step.

The hindcast has already shown its potential in building a statistical monitoring of the environment, with the objective of assessing variability and detecting changes in all its components and their spatial organisation (Woillez et al. 2010). In parallel, Petitgas et al. (2009) showed that the schedules of fish life cycles correspond to specific timing of the seasonal pattern, with for example anchovy larval development coinciding with low variability in the environment. Thus a monitoring procedure to

rapidly detect deviations from a typical seasonal pattern shows promising applications in the context of the Ecosystem Approach to Fisheries.

The hindcast maps may be used to derive fish habitats (Planque et al. 2007) from statistical regression of eggs or adult field distribution on environment covariates, and then extrapolate over unobserved seasons or years. The hindcast integrated 1D indices, when averaged over appropriate areas and periods in relation to the fish life cycles, can be tested them with statistical regression (Planque et al. 2008) in their ability to explain the recruitment as limiting factors.

Ecosystem modelling is progressively moving towards end-to-end modelling. Coupled physical-biogeochemical models are thus the basis for higher trophic level models. In a first step towards a real coupling, Struski et al. (2009) used the hindcast of the Bay of Biscay to force a bioenergetics adult growth and reproduction model, providing the variability in the spawning season and duration, the required starting point for Individual Based Models (IBMs) of larval transport and survival (Allain et al., 2007; Huret et al., 2010).

Acknowledgements

References

Allain, G., Petitgas, P., Lazure P. and Grellier, P. 2007. Biophysical modelling of larval drift, growth and survival for the prediction of anchovy (Engraulis encrasicolus) recruitment in the Bay of Biscay (NE Atlantic). Fisheries Oceanography, 16(6), 489-505.

Anonymous. 2008. Directive 2008/56/EC Marine Strategy Framework Directive. Official Journal of the European Union L164/19.

Bakun, A., 1996. *Patterns in the Ocean. Ocean processes and Marine Population Dynamics*, San Diego, CA, USA: University of California Sea Grant, in cooperation with Centro de Investigaciones Biologicas de Noroeste La Paz, Baja California Sur, Mexico, 323pp.

Berx, B., Dickey-Collas, M., Skogen, M.D., De Roeck, Y.-H., Klein, H., Barciela Fernandez, R., Foster, R., Gorringe, P., Vinay, G., Brostrøm, G., Dombrowsky, E., Huret, M., Legrand, E., Payne, M., Sagarminaga, Y., Schrum, C., Svendsen E. 2010. Does operational oceanography address the needs of fisheries and applied environmental scientists? In prep.

Chapelle A., Lazure P., et Menesguen A. 1994. Modelling eutrophication events in a coastal ecosystem – sensitivity analysis. Estuarine coastal and shelf science. 39(6): 529-548.

Chassot, E., Bonhommeau, S., Reygondeau, G., Nieto K., Polovina, J.J., Huret, M., Dulvy, N.K., Demarcq H. Satellite remote sensing for an Ecosystem Approach to Fisheries. ICES Journal of Marine Science. In revision.

Choi, B.J., Wilkin, J.L. (2007) The effect of wind on the dispersal of the Hudson river plume. Journal of Physical Oceanography, 37: 1878-1897.

Cury, P.M. et al., 2008. Ecosystem oceanography for global change in fisheries. *Trends In Ecology & Evolution*, 23(6), 338–346.

Dray, S., Dufour, A.-B., 2007. The ade4 package: Implementing the duality diagram for ecologists. Journal of Statistical Software 22(4), 1–20.

Guillaud J-F., 2008. Calcul en temps réel des concentrations fluviales en nutriments, en fonction des débits, sur la façade Atlantique, la Manche et le sud de la Mer du Nord. RST.DYNECO Pélagos 08-05.

Huret M., Gohin F., Delmas D., Lunven M., Garcon V. 2007. Use of SeaWiFS data for light availability and parameter estimation of a phytoplankton production model of the Bay of Biscay. Journal of Marine Systems. 65(1-4): 509-531.

Huret M., Petitgas P. and Woillez M. 2010. Dispersal kernels and their drivers captured with a hydrodynamic model and spatial indices : a case study on anchovy (Engraulis encrasicolus) early life stages in the Bay of Biscay. Progress in Oceanography, accepted.

Koutsikopoulos, C. and Le Cann, B. 1996. Physical processes and hydrological structures related to the Bay of Biscay anchovy. Scientia Marina, 60(2), 9-19.

Insern-Fontanet, J. , Garcia-Ladona, E., Font, J. 2006. Vortices of the Mediterranean Sea: An Altimetric Perspective. Journal of Physical Oceanography, 36: 87-103.

Lazure P., Dumas F. 2008. An external-internal mode coupling for a 3D hydrodynamical model for applications at regional scale (MARS). Advances in Water Resources. 31: 233-250.

Lazure P., Garnier V., Dumas F., Herry C., Chifflet M. 2009. Development of a hydrodynamic model of the Bay of Biscay. Validation of hydrology. Continental Shelf Research, 29: 985-997.

Le Pape O., Menesguen A. 1997. Hydrodynamic prevention of eutrophication in the Bay of Brest (France), a modelling approach. Journal of Marine Systems. 12: 171-186.

Levitus S., Boyer T. P., Conkright M. E., O' Brien T., Antonov J., Stephens C., Stathoplos L, Johnson D., Gelfeld R., 1998 : NOAA Atlas NESDIS 18,World Ocean Database 1998, U. S. Gov. Printing Office, Wash., D. C., 346pp + set of Cdroms.

Loyer S., 2001. Modélisation de la production phytoplanctonique dans la zone côtière atlantique enrichie par les apports fluviaux. Thèse de Doctorat. Université de Paris VI. 232 pp.

Lyard, F., Lefevre F., Letellier T. and Francis O. 2006. Modelling the global ocean tides: modern insights from FES2004. *Ocean Dynamics*, 56(5-6), 394–415.

Menesguen A., Cugier P., Leblond I., 2006. A new numerical technique for tracking chemical species in a multisource, coastal ecosystem applied to nitrogen causing Ulva blooms in the Bay of Brest (France). Limnology and Oceanography, 51(1): 591-601.

Michel, S., Vandermeirsch, F. and Lorance, P., 2009. Evolution of upper layer temperature in the Bay of Biscay during the last 40 years. *Aquatic living resources*, 22(4), 447-461.

Petitgas P., Huret M., Léger F., Peck M.A., Dickey-Collas M. and Rijnsdorp A.D. 2009. Patterns and schedules in hindcasted environments and fish life cycles. ICES CM 2009/E:25.

Planque B., Bellier, E. and Lazure, P. 2007. Modelling potential spawning habitat of sardine (Sardina pilchardus) and anchovy (Engraulis encrasicolus) in the Bay of Biscay. Fisheries Oceanography, 16: 16-30.

Planque B. and Buffaz L. 2008. Quantile regression models for fish recruitment-environment relationships : four case studies. Marine Ecology Progress Series, 357:213-223.

Reynaud T., P. Le Grand H. Mercier and Barnier B., 1998. A new analysis of hydrographic data in the Atlantic and its application to an inverse modeling study. *International WOCE Newsletter*, 32, 29-31.

Struski C., Petitgas, P. and Huret, M. 2009. Long-term hindcast and climate change forecast of habitat unsuitability using bioenergetics and physical-biogeochemical models: anchovy in the Bay of Biscay and the North Sea. ICES CM 2009/E:22.

Woillez M., Petitgas, P., Huret M., Struski C. and Léger F. 2010. Statistical monitoring of spatial patterns of environmental indices for integrated ecosystem assessment, application to the Bay of Biscay pelagic zone. Progress in Oceanography. Accepted.